



Fractional Quantum Hall Phase Transitions and Four-Flux States in Graphene

Benjamin E. Feldman,¹ Andrei J. Levin,¹ Benjamin Krauss,² Dmitry A. Abanin,^{1,3}
Bertrand I. Halperin,¹ Jurgen H. Smet,² and Amir Yacoby^{1,*}

¹*Department of Physics, Harvard University, Cambridge, Massachusetts 02138, USA*

²*Max-Planck-Institut für Festkörperforschung, Heisenbergstrasse 1, D-70569 Stuttgart, Germany*

³*Perimeter Institute for Theoretical Physics, Waterloo, Ontario N2L 6B9, Canada*

(Received 7 May 2013; published 16 August 2013)

Graphene and its multilayers have attracted considerable interest because their fourfold spin and valley degeneracy enables a rich variety of broken-symmetry states arising from electron-electron interactions, and raises the prospect of controlled phase transitions among them. Here we report local electronic compressibility measurements of ultraclean suspended graphene that reveal a multitude of fractional quantum Hall states surrounding filling factors $\nu = -1/2$ and $-1/4$. Several of these states exhibit phase transitions that indicate abrupt changes in the underlying order, and we observe many additional oscillations in compressibility as ν approaches $-1/2$, suggesting further changes in spin and/or valley polarization. We use a simple model based on crossing Landau levels of composite fermions with different internal degrees of freedom to explain many qualitative features of the experimental data. Our results add to the diverse array of many-body states observed in graphene and demonstrate substantial control over their order parameters.

DOI: [10.1103/PhysRevLett.111.076802](https://doi.org/10.1103/PhysRevLett.111.076802)

PACS numbers: 73.22.Pr, 73.43.-f

When a two-dimensional electron gas is subject to a perpendicular magnetic field B , the electronic spectrum forms a sequence of Landau levels (LLs). Generally, this gives rise to incompressible quantized Hall states at integer values of the filling factor $\nu = nh/eB$, where n is the carrier density, h is Planck's constant, and e is the electron charge. In very clean samples at high magnetic field, Coulomb interactions become important and produce additional quantized Hall states at certain fractional filling factors [1–4]. These fractional quantized Hall (FQH) states can be understood in terms of composite fermions (CFs), which may be described as an electron bound to an even number m of magnetic flux quanta. CFs experience a reduced effective magnetic field, and FQH states at $\nu = p/(mp \pm 1)$ are understood to arise when an integer number p of m CF LLs are occupied. In CF theory, FQH states of electrons are therefore interpreted as the integer quantized Hall effect of these new composite particles [4].

Like electrons, CFs can have internal quantum numbers such as spin or valley index (isospin). When more than one CF LL is occupied, ground states with different polarizations of these degrees of freedom are possible at a given filling factor, and transitions between different phases may occur when system parameters are varied. Phase transitions between FQH states with differing spin polarization have been observed in GaAs by tuning the magnitude of the magnetic field [5–8], its direction [9–14], or the applied pressure [15]. In AlAs 2DEGs, strain has been used to induce phase transitions between valley-polarized and unpolarized states [16–18].

In graphene, the electronic Hamiltonian has an approximate SU(4) symmetry arising from the spin and valley degrees of freedom. This symmetry is weakly broken due to the Zeeman effect and electron-electron scattering

between valleys, which may be enhanced by (or compete with) effects of the dominant Coulomb interactions. Electron-electron interactions were recently shown to produce surprising patterns of symmetry breaking and phase transitions in the integer quantum Hall regime [19–23]. Theoretical proposals suggest that the strengths of FQH states can also be tuned in monolayer and bilayer graphene, and that transitions between different ordered phases are possible [24–26]. However, despite the observation of robust FQH states in graphene [27–32], their rich phase diagram has yet to be fully explored.

Here we report local electronic compressibility measurements of suspended graphene, performed using a scanning single-electron transistor (SET) [33,34]. A schematic of the measurement setup [35] is shown in Fig. 1(a). Modulating the carrier density with a back gate and monitoring the resulting change in SET current allows us to measure both the local chemical potential μ and the local inverse compressibility of the graphene flake with a spatial resolution of about 100 nm. The inverse compressibility κ^{-1} is properly defined as $n^2 d\mu/dn$, but hereafter we drop the prefactor and use the term to mean $d\mu/dn$. The data presented below were taken at one location, but similar behavior was observed at multiple positions [35].

Figure 1(b) shows the inverse compressibility as a function of filling factor and magnetic field. FQH states appear as vertical incompressible peaks at $\nu = -1/3, -2/3, -2/5, -3/5, -3/7, -4/7, -4/9, -5/9$, and $-5/11$, consistent with the standard CF sequence observed for $|\nu| < 1$ in previous measurements [32]. Surprisingly, every FQH state except $\nu = -1/3$ exhibits a narrow magnetic field range over which the incompressible behavior is strongly suppressed. The critical field at which this occurs increases with filling fraction denominator, and the suppression is

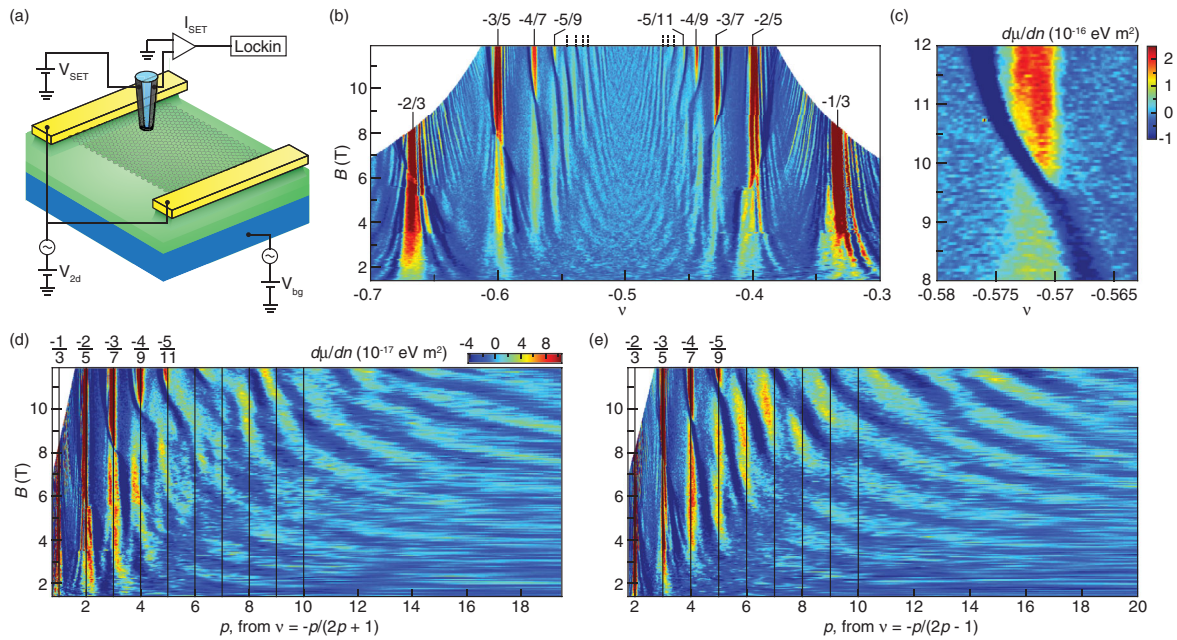


FIG. 1 (color). (a) Schematic of the measurement setup. (b) Inverse compressibility $d\mu/dn$ as a function of filling factor ν and magnetic field B . (c) Finer measurement around $\nu = -4/7$. Panels (b) and (c) have identical color scales. (d) and (e) $d\mu/dn$ as a function of B and composite fermion Landau level (CF LL) index p . Panels (d) and (e) have identical color scales. Principal FQH states are marked by black lines and are labeled. The dashed lines in panel (b) mark where higher-denominator FQH states in the standard CF sequence would be expected to occur.

associated with regions of sharply negative compressibility that cross each FQH state, often generating two coexisting incompressible peaks at slightly different filling factors over a small range in magnetic field [Fig. 1(c)]. Interestingly, the negative compressibility has an especially large amplitude that is similar (but opposite in sign) to the incompressible peaks of the actual FQH states.

The interruptions in each incompressible peak suggest phase transitions in which the spin and/or valley polarization of electrons changes abruptly. The behavior is similar to that observed in GaAs, where transport measurements showed FQH states splitting into doublets near phase transitions [6,7,11,14]. However, no dramatic features of negative compressibility were present in GaAs [8], and the inverse compressibility did not display a strong asymmetry between filling factors just above and below the FQH states [8,36].

Several less prominent modulations in compressibility that occur close to $\nu = -1/2$ are also visible in Fig. 1(b). We emphasize that they are not caused by localized states, which occur near the strongest FQH states such as $\nu = -2/3$, but not around high-denominator states, such as $\nu = -4/7$ [35]. Further insight can be gained by plotting the inverse compressibility as a function of p rather than ν [Figs. 1(d) and 1(e)]. This more clearly illustrates the behavior near $\nu = -1/2$ and reveals oscillations in inverse compressibility that persist to values of p as large as 20 and magnetic fields as low as a few Tesla. The behavior cannot be explained by Shubnikov–de Haas oscillations of CFs, because variations in compressibility occur even at

constant filling factor. The oscillations become stronger and more vertical as the magnetic field is increased, suggesting that they are associated with developing FQH states. Moreover, they seem to extend from the negative compressibility features of the phase transitions, suggesting that they result from changes in spin and/or valley polarization as magnetic field and filling factor are varied.

Signatures of phase transitions have previously been observed in compressibility measurements only at $\nu = 2/3$ in GaAs [8], although optical and transport studies of GaAs and AlAs have revealed evidence of changes in spin or isospin polarization for filling fractions with larger denominators [9,37]. We observe clear phase transitions up to $\nu = -5/9$ and $-5/11$, and additional compressibility oscillations are apparent much closer to $\nu = -1/2$. Similar oscillations have not been reported in GaAs; their existence in graphene suggests a rich array of ordered electronic states and hints at a delicate energetic competition among them.

To gain further insight, we introduce a simple model to describe CFs with internal degrees of freedom [38–41] (see [35] for details). Because of graphene’s peculiar band structure, the lowest LL is already half full at $\nu = 0$, and experiments suggest that the $\nu = 0$ state has no net spin polarization [19]. For $0 > \nu > -1$, we assume that the ground state is obtained by putting holes in the $\nu = 0$ state, which we convert to CFs by attaching two flux quanta to each hole. The CFs have two possible spin states (\pm) and we consider many-body states where there may be different particle densities for the two spins. Single-particle

energies of the two spin states will be split by an amount proportional to B due to the Zeeman effect, which favors a spin-polarized state. However, the $SU(4)$ invariant part of the Coulomb interaction will typically favor states with more equal occupation of spins [39]. Because the Coulomb interaction energies scale as $B^{1/2}$, then for fixed ν , varying the magnetic field will change the relative importance of the two terms, which suggests that the experimentally observed phase transitions may be caused by changes in spin polarization, as in GaAs.

Our model applies most directly to the situation where all electrons in the ground state of $\nu = 0$ have the same valley configuration, as in the Kekule or the charge-density-wave states [42]. The antiferromagnetic state is more complicated because the constituent electron states differ in valley index as well as spin, but we expect that results for this case should be at least qualitatively similar to the case we consider [43]. Future studies in which a tilted magnetic field is applied to the sample may help determine the spin and valley ordering of the FQH states.

Within our model, effects of the $SU(4)$ invariant Coulomb interaction are modeled by a sum of the “kinetic energies” of the occupied states in the CF LLs, which scale as $B^{1/2}$ for fixed orbital index N^* . A schematic diagram of CF LL energies $E_{N^*}^{\pm}$ and their scaling with magnetic field is shown in Fig. 2(a). At certain critical magnetic fields, CF LLs with different spin and orbital degrees of freedom cross, leading to phase transitions.

Based on this model, we have numerically simulated the inverse compressibility. In our simulation, we broaden the CF LLs by a fixed amount of disorder δn and calculate the occupation of each CF LL, which ultimately yields the inverse compressibility as a function of density and magnetic field. The results, which assume either a small amount of disorder or more realistic density fluctuations based on the widths of the FQH peaks, are shown in Figs. 2(b) and 2(c), respectively.

The simulations in Fig. 2 share many characteristics with the experimental data. Most striking are the breaks in the incompressible peaks of FQH states with $p \geq 2$. In addition, the simulations show regions of negative compressibility that cross from one side of the FQH state to the other as the phase transition occurs. This is qualitatively similar to the behavior that we observe, although the experimental features are much narrower. Finally, the oscillations in inverse compressibility become less robust and start to curve at low magnetic field and high p , similar to the experimental data. The values used for parameters in the simulation agree well with expectations based on other experimental metrics. By matching the simulation to the experimental critical fields and assuming Zeeman splitting with a g factor of 2, we extract an effective mass $m^* = 0.18m_e(\nu B[T])^{1/2}$, the same order of magnitude as for CFs in GaAs [5]. In addition, the density fluctuations $\delta n = 1.5 \times 10^8 \text{ cm}^{-2}$ assumed in Fig. 2(c) are comparable to the widths of the FQH states we observe. Given the simplicity

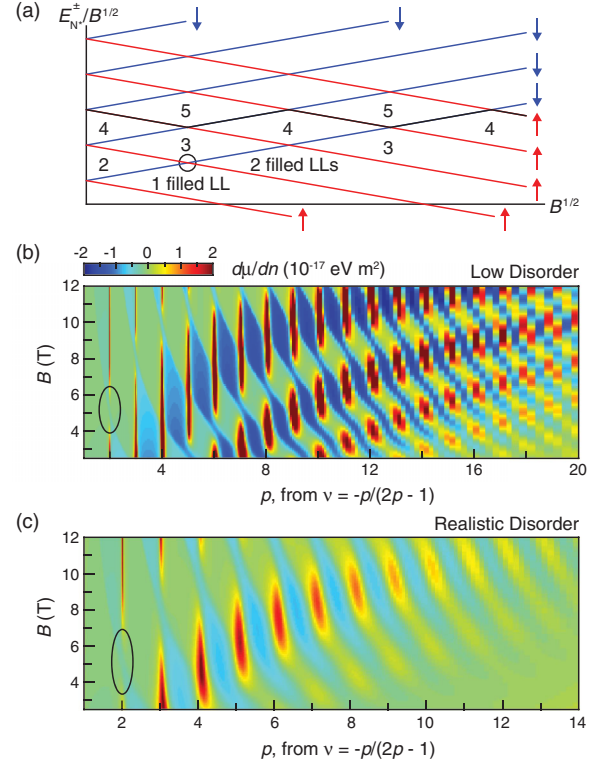


FIG. 2 (color). (a) Schematic of CF LL energies E_p^{\pm} divided by and plotted against $B^{1/2}$. Crossings (black circle) between spin-up and -down CF LLs (colored arrows) correspond to phase transitions. (b) and (c) Numerical simulations of $d\mu/dn$ as a function of B and p assuming either minimal charge inhomogeneity (b), or more realistic density fluctuations (c). Black ovals correspond to the black circle in panel (a). Both panels use the same color scale.

of the model, the agreement with experiment is remarkable, suggesting that it provides a basic framework to understand the underlying physics.

The critical fields of the phase transitions vary slightly with position, and a much smaller critical field at $\nu = 2/3$ was observed before the final current annealing step [35]. The change after current annealing suggests that disorder is relevant, but the exact mechanism is not clear. Disorder that breaks valley symmetry could preferentially support one FQH phase over the other if the $\nu = 0$ state is a canted antiferromagnet. It is also possible that the level of disorder affects the dielectric constant. The origin of the spatial dependence merits further study.

Integrating the inverse compressibility with respect to carrier density allows us to extract the steps in chemical potential $\Delta\mu_{\nu}$ of each FQH state; multiplying $\Delta\mu_{\nu}$ by the quasiparticle charge then yields the corresponding energy gaps. Figures 3(a) and 3(b) show inverse compressibility and chemical potential, respectively, as a function of filling factor at 11.9 T. In Figs. 3(c) and 3(d), we plot $\Delta\mu_{\nu}$ as a function of magnetic field. The complex nonmonotonic behavior of the energy gaps exhibited by several FQH states [Fig. 3(d)] is similar to the behavior in GaAs near

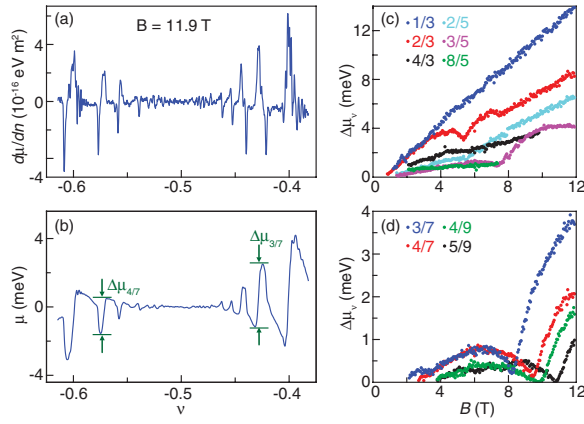


FIG. 3 (color). $d\mu/dn$ (a) and chemical potential μ relative to its value at $\nu = -1/2$ (b) as a function of ν at $B = 11.9$ T. (c) and (d) Steps in chemical potential $\Delta\mu_\nu$ [green labels in panel (b)] of FQH states as a function of B at measured multiples of $\nu = 1/3$ and $1/5$ (c), and $\nu = 1/7$ and $1/9$ (d).

phase transitions [13]. This behavior becomes increasingly pronounced and the field range over which incompressible behavior is suppressed widens as filling factor denominator increases. A similar pattern occurs in the simulations of Fig. 2, and it likely results from the increasing effects of density fluctuations on CF LL width as p increases.

The step in chemical potential at $\nu = -1/3$ scales linearly with B over the entire field range that we study. This behavior is consistent with prior studies [32], but the linearity is surprising because interaction-driven states typically scale as $B^{1/2}$. The behavior also contradicts the $B^{1/2}$ dependence expected from our model, although we note that the model does not include interactions among CFs, LL mixing, finite temperature effects, or the possibility of other excitations such as Skyrmions. Linear scaling with magnetic field at $\nu = 1/3$ has been theoretically predicted to arise from spin-flip excitations over an intermediate field range [44].

In addition to the phase transitions discussed above, the exceptional sample quality reveals several FQH states belonging to the ${}^4\text{CF}$ sequence $\nu = p/(4p \pm 1)$ and its analogue around $\nu = -1$. We observe incompressible behavior at $\nu = -1/5, -2/7, -2/9, -3/11, -5/7$ and $-6/5$ [Figs. 4(a)–4(c)]. An additional weak incompressible peak occurs between $\nu = -9/7$ and $-14/11$, but the experimental uncertainty in filling factor prevents a more precise assignment [35]. No other ${}^4\text{CF}$ states are visible; FQH states at $\nu = -4/5, -9/5$, and $-12/7$ are conspicuously absent, despite the robust appearance of their counterparts near $\nu = 0$. This may reflect interesting patterns of symmetry breaking in the lowest LL [35,45], but could also be caused by differing degrees of disorder at different filling factors, or by competition with other quantum Hall states, particularly near $\nu = -2$.

The extracted steps in chemical potential for several ${}^4\text{CF}$ FQH states are plotted as a function of magnetic field

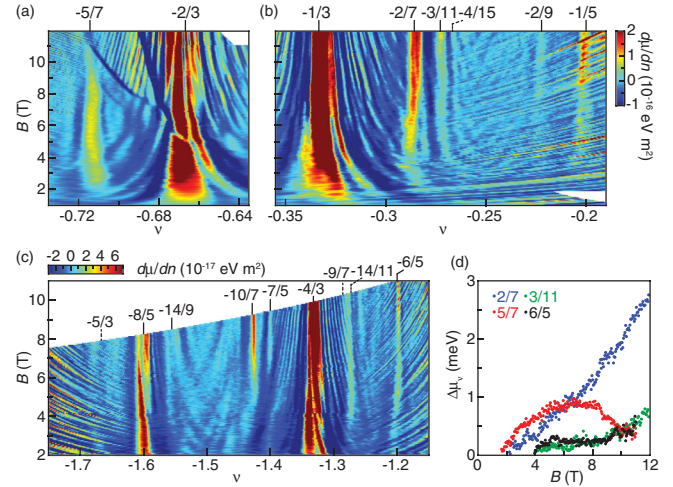


FIG. 4 (color). (a)–(c) $d\mu/dn$ as a function of ν and B . Prominent four-flux FQH states are labeled. (d) $\Delta\mu_\nu$ of the ${}^4\text{CF}$ states as a function of B .

in Fig. 4(d). The fluctuations caused by localized states near $\nu = -1/5$ and $-2/9$ prevent an accurate determination of $\Delta\mu_\nu$ for these states, but all other states except for $\nu = -5/7$ scale approximately linearly with magnetic field. Further study is required to determine whether the nonmonotonic behavior of $\Delta\mu_{-5/7}$ reflects a phase transition or whether the state is simply competing with $\nu = -2/3$. Regardless, the appearance of ${}^4\text{CF}$ states and phase transitions represents an important advance in sample quality that enables further study of and control over the delicate many-body states arising from interacting Dirac fermions in graphene.

We would like to thank M. T. Allen for help with current annealing. We also acknowledge useful discussions with M. Kharitonov, J. K. Jain, L. S. Levitov, and S. H. Simon. This work is supported by the U.S. Department of Energy, Office of Basic Energy Sciences, Division of Materials Sciences and Engineering under Award No. DE-SC0001819. J. H. S. and B. K. acknowledge financial support from the DFG graphene priority programme. B. K. acknowledges financial support from the Bayer Science and Education Foundation. This work was performed in part at the Center for Nanoscale Systems at Harvard University, a member of the National Nanotechnology Infrastructure Network, which is supported by the National Science Foundation under Award No. ECS-0335765.

*yacoby@physics.harvard.edu

- [1] D. C. Tsui, H. L. Stormer, and A. C. Gossard, *Phys. Rev. Lett.* **48**, 1559 (1982).
- [2] R. B. Laughlin, *Phys. Rev. Lett.* **50**, 1395 (1983).
- [3] B. I. Halperin, *Helv. Phys. Acta* **56**, 75 (1983).
- [4] J. K. Jain, *Phys. Rev. Lett.* **63**, 199 (1989).
- [5] I. V. Kukushkin, K. von Klitzing, and K. Eberl, *Phys. Rev. Lett.* **82**, 3665 (1999).

- [6] J.H. Smet, R.A. Deutschmann, W. Wegscheider, G. Abstreiter, and K. von Klitzing, *Phys. Rev. Lett.* **86**, 2412 (2001).
- [7] J.H. Smet, R.A. Deutschmann, F. Ertl, W. Wegscheider, G. Abstreiter, and K. von Klitzing, *Nature (London)* **415**, 281 (2002).
- [8] B. Verdene, J. Martin, G. Gamez, J. Smet, K. von Klitzing, D. Mahalu, D. Schuh, G. Abstreiter, and A. Yacoby, *Nat. Phys.* **3**, 392 (2007).
- [9] R.R. Du, A.S. Yeh, H.L. Stormer, D.C. Tsui, L.N. Pfeiffer, and K.W. West, *Phys. Rev. Lett.* **75**, 3926 (1995).
- [10] M. Chen, W. Kang, and W. Wegscheider, *Phys. Rev. Lett.* **91**, 116804 (2003).
- [11] J.P. Eisenstein, H.L. Stormer, L. Pfeiffer, and K.W. West, *Phys. Rev. Lett.* **62**, 1540 (1989).
- [12] R.G. Clark, S.R. Haynes, A.M. Suckling, J.R. Mallett, P.A. Wright, J.J. Harris, and C.T. Foxon, *Phys. Rev. Lett.* **62**, 1536 (1989).
- [13] J.P. Eisenstein, H.L. Stormer, L.N. Pfeiffer, and K.W. West, *Phys. Rev. B* **41**, 7910 (1990).
- [14] L.W. Engel, S.W. Hwang, T. Sajoto, D.C. Tsui, and M. Shayegan, *Phys. Rev. B* **45**, 3418 (1992).
- [15] H. Cho, J.B. Young, W. Kang, K.L. Campman, A.C. Gossard, M. Bichler, and W. Wegscheider, *Phys. Rev. Lett.* **81**, 2522 (1998).
- [16] N.C. Bishop, M. Padmanabhan, K. Vakili, Y.P. Shkolnikov, E.P. De Poortere, and M. Shayegan, *Phys. Rev. Lett.* **98**, 266404 (2007).
- [17] M. Padmanabhan, T. Gokmen, and M. Shayegan, *Phys. Rev. Lett.* **104**, 016805 (2010).
- [18] M. Padmanabhan, T. Gokmen, and M. Shayegan, *Phys. Rev. B* **81**, 113301 (2010).
- [19] A.F. Young, C.R. Dean, L. Wang, H. Ren, P. Cadden-Zimansky, K. Watanabe, T. Taniguchi, J. Hone, K.L. Shepard, and P. Kim, *Nat. Phys.* **8**, 550 (2012).
- [20] R.T. Weitz, M.T. Allen, B.E. Feldman, J. Martin, and A. Yacoby, *Science* **330**, 812 (2010).
- [21] S. Kim, K. Lee, and E. Tutuc, *Phys. Rev. Lett.* **107**, 016803 (2011).
- [22] J. Velasco *et al.*, *Nat. Nanotechnol.* **7**, 156 (2012).
- [23] P. Maher, C.R. Dean, A.F. Young, T. Taniguchi, K. Watanabe, K.L. Shepard, J. Hone, and P. Kim, *Nat. Phys.* **9**, 154 (2013).
- [24] V.M. Apalkov and T. Chakraborty, *Phys. Rev. Lett.* **105**, 036801 (2010).
- [25] Z. Papic, D.A. Abanin, Y. Barlas, and R.N. Bhatt, *Phys. Rev. B* **84**, 241306 (2011).
- [26] Z. Papic, R. Thomale, and D.A. Abanin, *Phys. Rev. Lett.* **107**, 176602 (2011).
- [27] C.R. Dean, A.F. Young, P. Cadden-Zimansky, L. Wang, H. Ren, K. Watanabe, T. Taniguchi, P. Kim, J. Hone, and K.L. Shepard, *Nat. Phys.* **7**, 693 (2011).
- [28] X. Du, I. Skachko, F. Duerr, A. Luican, and E.Y. Andrei, *Nature (London)* **462**, 192 (2009).
- [29] K.I. Bolotin, F. Ghahari, M.D. Shulman, H.L. Stormer, and P. Kim, *Nature (London)* **462**, 196 (2009).
- [30] F. Ghahari, Y. Zhao, P. Cadden-Zimansky, K. Bolotin, and P. Kim, *Phys. Rev. Lett.* **106**, 046801 (2011).
- [31] D.S. Lee, V. Skakalova, R.T. Weitz, K. von Klitzing, and J.H. Smet, *Phys. Rev. Lett.* **109**, 056602 (2012).
- [32] B.E. Feldman, B. Krauss, J.H. Smet, and A. Yacoby, *Science* **337**, 1196 (2012).
- [33] M.J. Yoo, T.A. Fulton, H.F. Hess, R.L. Willett, L.N. Dunkleberger, R.J. Chichester, L.N. Pfeiffer, and K.W. West, *Science* **276**, 579 (1997).
- [34] A. Yacoby, H.F. Hess, T.A. Fulton, L.N. Pfeiffer, and K.W. West, *Solid State Commun.* **111**, 1 (1999).
- [35] See Supplemental Material at <http://link.aps.org/supplemental/10.1103/PhysRevLett.111.076802> for a detailed model description, additional data, and methods.
- [36] J.P. Eisenstein, L.N. Pfeiffer, and K.W. West, *Phys. Rev. B* **50**, 1760 (1994).
- [37] M. Padmanabhan, T. Gokmen, and M. Shayegan, *Phys. Rev. B* **80**, 035423 (2009).
- [38] K. Park and J.K. Jain, *Phys. Rev. Lett.* **80**, 4237 (1998).
- [39] C. Toke and J.K. Jain, *J. Phys. Condens. Matter* **24**, 235601 (2012).
- [40] C. Toke and J.K. Jain, *Phys. Rev. B* **75**, 245440 (2007).
- [41] K. Yang, S. Das Sarma, and A.H. MacDonald, *Phys. Rev. B* **74**, 075423 (2006).
- [42] M. Kharitonov, *Phys. Rev. B* **85**, 155439 (2012).
- [43] D.A. Abanin, B.E. Feldman, A. Yacoby, and B.I. Halperin, [arXiv:1303.5372v1](https://arxiv.org/abs/1303.5372v1).
- [44] Z. Papic, M.O. Goerbig, and N. Regnault, *Phys. Rev. Lett.* **105**, 176802 (2010).
- [45] T.M. Kott, B. Hu, S.H. Brown, and B.E. Kane, [arXiv:1210.2386v1](https://arxiv.org/abs/1210.2386v1).